RSC Advances

PAPER

View Article Online
View Journal | View Issue

Cite this: *RSC Adv.*, 2014, **4**, 27159

Transcriptome-wide identification and characterization of *Ornithogalum saundersiae* phenylalanine ammonia lyase gene family†

Zhi-Biao Wang, Xi Chen, Wei Wang, Ke-Di Cheng and Jian-Qiang Kong*

Received 14th April 2014
Accepted 21st May 2014

DOI: 10.1039/c4ra03385j

www.rsc.org/advances

OSW-1 is a promising antitumor glycoside present in the *Ornithogalum saundersiae* plant. Biosynthesis of the *p*-methoxybenzoyl group on the disaccharide moiety of OSW-1 is known to take place biochemically by phenylpropanoid biosynthetic pathway, but molecular biological characterization of related genes has been insufficient. Phenylalanine ammonia lyase (PAL, EC 4.3.1.24), which catalyzes the deamination of L-phenylalanine to yield *trans*-cinnamic acid, plays a key role in phenylpropanoid metabolism. Thus, the study on the characterization of the genes involved in the OSW-1 biosynthetic pathway, particularly the well-documented genes such as PAL, is essential to further the understanding of the biosynthesis of OSW-1. Here, transcriptomic sequencing of *O. saundersiae* was performed to speed up the identification of a large number of genes related to OSW-1 biosynthesis. *De novo* assembly of the transcriptome sequence provided 210 733 contigs, 104, 180 unigenes, and four unigenes showing high similarities with PALs. Two full-length cDNAs encoding PALs (*OsaPAL2* and *OsaPAL62*) from *O. saundersiae* were cloned using sequence information from these four unigenes. The PAL and tyrosine ammonia lyase (TAL) activities of recombinant OsaPAL proteins were unambiguously determined by HPLC with UV and MS detection as well as by NMR spectroscopy. Subsequently, a series of site-directed mutants were generated with the aim of improving enzyme activity and investigating the importance of particular residues in determining substrate selectivity. The results reveal that the Phe-to-His mutants, *i.e.*, OsaPAL2F134H and OsaPAL62F128H, exhibited higher TAL activity than the corresponding wild types, providing direct evidence that the Phe residue is responsible for substrate specificity. Mutagenesis studies also demonstrated that the Thr-to-Ser mutants, *i.e.*, OsaPAL2T196S and OsaPAL62T194S, showed significantly higher substrate affinity than the wild types. Furthermore, the Gly-to-Ala mutants, *i.e.*, OsaPAL2G209A and OsaPAL62G207A, showed higher PAL and TAL activities. These findings provide further insight into the genes responsible for OSW-1 biosynthesis and will facilitate the future application of OsaPALs in synthetic biology.

1. Introduction

Phenylalanine ammonia lyase (PAL, EC 4.3.1.24), a member of the superfamily of ammonia lyases, catalyzes the conversion of L-phenylalanine to *trans*-cinnamic acid by a non-oxidative deamination. In recent years, considerable attention has been paid to the presence of PALs in medicinal plants since they are involved in the biosynthesis of the majority of phenol-containing secondary metabolites, many of which are pharmacologically active.[1,2]

OSW-1 (Fig. 1A), which is a natural saponin isolated from *Ornithogalum saundersiae*, exhibits exceptionally potent antitumor activity both *in vitro* and *in vivo*.[3–5] As such, it is a promising lead compound for the development of novel antitumor drugs; however, because of its low content in the plant and a long and laborious synthesis,[6–10] little progress has been made in developing OSW-1 as a potential drug candidate after its discovery in 1992.[11] Accordingly, we have initiated a project to identify an alternative, preparative-scale method to produce OSW-1 and to elucidate its biosynthetic pathway and the enzymes involved.

OSW-1 is characterized by a disaccharide moiety attached to the C-16 position of the steroid aglycone, which contains a *p*-methoxybenzoyl (MBz) and an acetyl (Ac) group.[11] According to previous structure–activity relationship (SAR) studies, the disaccharide moiety is important for the cytotoxicity of OSW-1 and, in particular, the removal of the Ac and MBz groups decreases the activity of OSW-1 by approximately 1000-fold.[3,12,13]

Institute of Materia Medica, Chinese Academy of Medical Sciences & Peking Union Medical College (State Key Laboratory of Bioactive Substance and Function of Natural Medicines & Ministry of Health Key Laboratory of Biosynthesis of Natural Products), Beijing, 100050, China. E-mail: jianqiangk@imm.ac.cn; Tel: +86-10-63165169

† Electronic supplementary information (ESI) available. See DOI: 10.1039/c4ra03385j

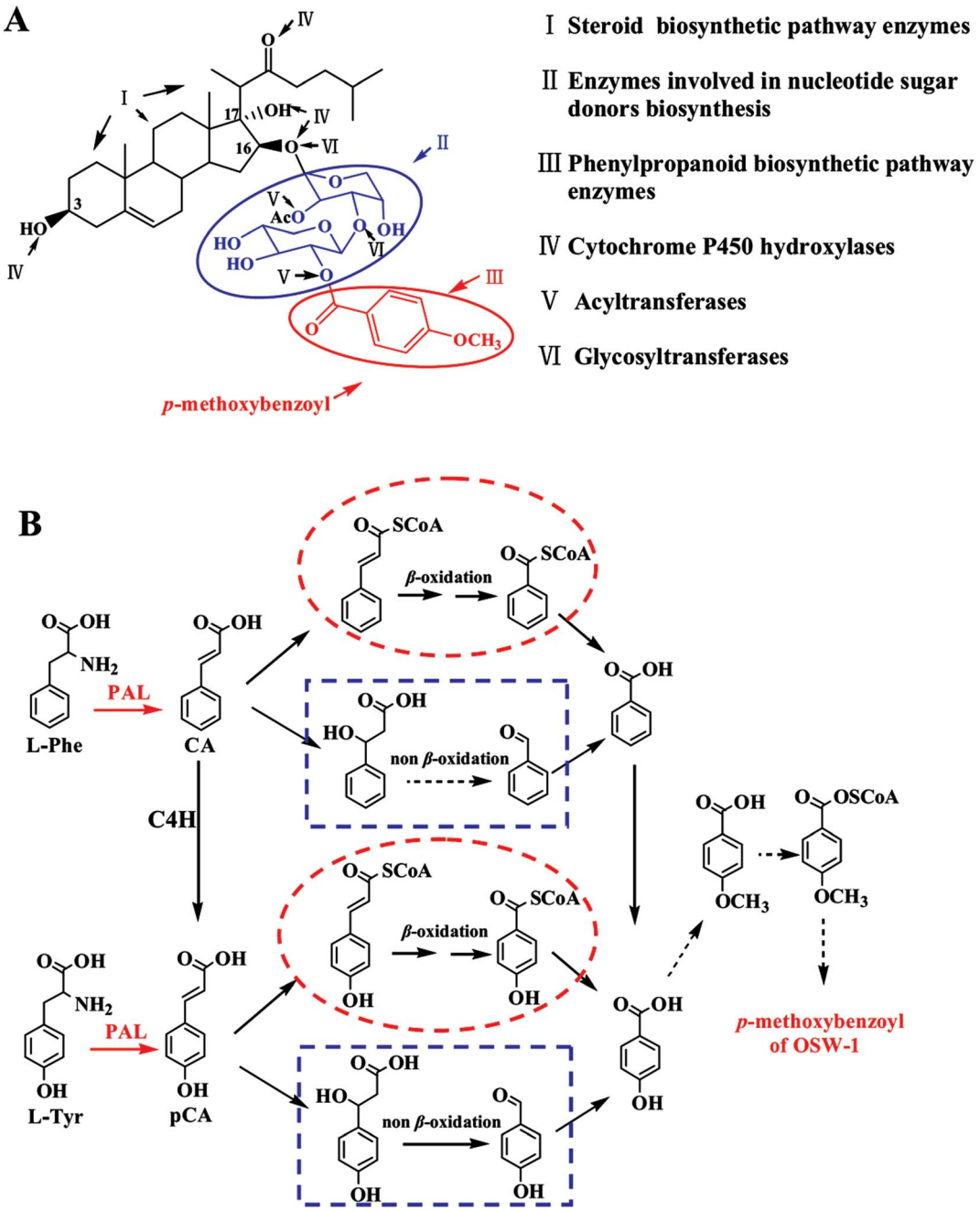

Fig. 1 (A) The structure of OSW-1 with the *p*-methoxybenzoyl group (dashed circle) and the enzymes responsible for OSW-1 biosynthesis. (B) The proposed pathways for the biosynthesis of the *p*-methoxybenzoyl group. Dashed circles show the β-oxidation pathway and dashed boxes show the non β-oxidation pathway. Solid arrows show the established biochemical steps and broken arrows show the hypothetical steps. Stacked arrows indicate the involvement of multiple enzymatic reactions. (PAL, phenylalanine ammonia lyase; C4H, cinnamate-4-hydroxylase; TAL, tyrosine ammonia lyase; CA, *trans*-cinnamic acid; pCA, *p*-coumaric acid).

Many previous studies have indicated that the *p*-hydroxybenzoic acid group is derived either from L-Phe or L-Tyr (Fig. 1B) through the respective PAL-catalyzed formation of *trans*-cinnamic acid or *p*-coumaric acid.[14–16] Thus, it is likely that PALs play an important role in this phenylpropanoid biosynthetic pathway for OSW-1; however, to date, none of the PALs in *O. saundersiae* have been cloned or characterized.

PAL was first purified from *Hordeum vulgare* in 1961,[17] and it was later found to be widespread in plants,[18–20] fungi[21–23] and prokaryotes.[24–26] In plants, PALs are fairly ubiquitous; moreover, they can be found in monocots,[27–30] dicots,[1,18,19,31] gymnosperms,[32–35] ferns,[36] lycopods,[36] liverworts,[36] and algae;[37] however, there are no reports about PALs in the Asparagaceae species.

Here, a gene family containing two OsaPAL genes was isolated for the first time from an Asparagaceae plant, *O. saundersiae*. After a successful functional characterization, a series of site-directed mutants were generated with the aim of

improving enzyme activity and investigating the importance of specific residues in determining substrate selectivity. The *in vitro* assays indicated that we successfully improved both the PAL and TAL deamination activities of OsaPALs using a single amino acid substitution, a discovery that we believe will provide additional ways to improve PAL activity of other such enzymes. We also believe that a greater understanding of how OsaPALs participate in the biosynthesis of OSW-1 will facilitate future applications of OsaPALs in synthetic biology.

2. Experimental methods

2.1. Substrates, chemicals and enzymes

Materials (suppliers) used in this study were as follows: L-Phe and L-Tyr were used in the enzyme assays (Sigma-Aldrich Co. Ltd., St. Louis, MO, USA); In-Fusion® HD Cloning Kit, restriction enzymes (Takara Shuzo Co. Ltd., Kyoto, Japan) and Super RT cDNA Kit were used to synthesize full-length cDNAs and KOD-Plus-Neo DNA polymerases (Toyobo Co. Ltd., Osaka, Japan); RNeasy Plant Mini Kit was used for RNA extraction (Qiagen, Dusseldorf, Germany); Ni-Sepharose (Invitrogen, Carlsbad, CA, USA) and Fast Mutagenesis System kit were used for the site-directed mutagenesis (TransGen Biotech Co. Ltd., Beijing, China). All other chemicals used in this study were of analytical grade.

2.2. Strains and plasmids

Prokaryotic expression vector, *i.e.* pET-28a (+), which was used for heterologous expression, was purchased from Novagen, Madison, USA. Expression host strain *Transetta* (DE3) and the cloning vector *pEASY*®-Blunt were purchased from TransGen Biotech Co. Ltd., Beijing, China. TG1 was used as a bacterial host for recombinant plasmid amplification. The host was grown in Luria–Bertani medium (10 g l^{-1} Bacto-Tryptone, 5 g l^{-1} Bacto-yeast extract, 10 g l^{-1} NaCl) or induced in TB medium (12 g l^{-1} Bacto-Tryptone, 24 g l^{-1} Bacto-yeast extract, 4 ml l^{-1} glycerol, 72 mM K_2HPO_4, 17 mM KH_2PO_4) supplemented with appropriate antibiotics for selection.

2.3. Plant materials

O. saundersiae was grown under sterile conditions on 6,7-V medium[38] at a temperature of 22 °C under a 16 h light/8 h dark cycle. Sterile bulbs were collected and used immediately for RNA isolation.

2.4. Transcriptome sequencing and analysis

RNA extraction and cDNA library construction were performed as described in Kong *et al.*[39] The resultant cDNA library was sequenced using Illumina HiSeq™ 2000. Short nucleotide reads obtained *via* Illumina sequencing were assembled using the Trinity software (http://www.trinity-software.com) to produce error-free, unique contiguous sequences (contigs). These contigs were ligated to obtain non-redundant unigenes, which could not be extended on either end. Unigene sequences were aligned by Blast X to protein databases like NCBI nr, Swiss-Prot, KEGG and COG (e-value < 0.00001), and aligned by Blast N to nucleotide databases nt (e-value < 0.00001), resulting in proteins with the highest sequence similarity with the given unigenes along with their functional annotations.

2.5. Generation of full-length OsaPALs cDNA and sequence analysis

Because the assembled sequences were products of *de novo* assemblies, they were considered prone to error. To confirm whether a sequence represented a true gene product, experimental verification was performed by designing gene-specific primers (Table 1) for the *OsaPAL* full-length sequences, and then verifying the identity of amplified products by sequencing.

Total RNA isolated from sterile bulb tissue of *O. saundersiae* using an RNeasy Plant Mini Kit (Qiagen) was used as a template for reverse transcription with primer oligo $(dT)_{20}$ primers and reverse transcriptase ReverTra Ace (TOYOBO) according to the manufacturer's instructions. The amplification of *OsaPAL*

Table 1 Primers used in gene cloning and plasmid construction

Primers	Sequences (5′–3′)	Description
FPAL1	5′-CATCATAATCTGACGGTTTTC-3′	Forward primer used for *OsaPAL2* amplification in the first round
FPAL2	5′-ATGGAGAACGGCAACGGTAA-3′	Forward primer used for *OsaPAL2* amplification in the second round
RPAL3	5′-CAGAATTATGAAATTCCAGCC-3′	Reverse primer used for *OsaPAL2* amplification in the first round
RPAL4	5′-TCAACATATTGGCAGCGGTGC-3′	Reverse primer used for *OsaPAL2* amplification in the second round
FET28aPAL2	5′-TCGCGGATCCGAATTCATGGAGA ACGGCAACGGTAAC-3′	Forward primer used for pET28a–OsaPAL2 construction
RET28aPAL2	5′-GTGCGGCCGCAAGCTTTCAACATA TTGGCAGCGGTGC-3′	Reverse primer used for pET28a–OsaPAL2 construction
FPAL5	5′-CAATCAGCCGTTTACGAGACC-3′	Forward primer used for *OsaPAL62* amplification in the first round
FPAL6	5′-ATGGAATCCCTCCACGCCAAC-3′	Forward primer used for *OsaPAL62* amplification in the second round
RPAL1	5′-CCGAAGTACTGAATGAAAATC-3′	Reverse primer used for *OsaPAL62* amplification in the first round
RPAL2	5′-CTAGCAAATGGGCAGGGGAG-3′	Reverse primer used for *OsaPAL62* amplification in the second round
FET28aPAL62	5′-TCGCGGATCCGAATTCATGGAAT CCCTCCACGCCAAC-3′	Forward primer used for pET28a–OsaPAL62 construction
RET28aPAL62	5′-GTGCGGCCGCAAGCTTCTAGCA AATGGGCAGGGGAG-3′	Reverse primer used for pET28a–OsaPAL62 construction

cDNAs was performed by a nested PCR method using KOD Plus Taq polymerase and gene-specific primers (Table 1). The amplified full-length cDNAs, *i.e.*, *OsaPAL2* and *OsaPAL62*, were each inserted into the *pEASY*®-Blunt vector to generate pEASY-OsaPAL2 and pEASY-OsaPAL62, respectively, for sequencing.

OsaPAL2 and *OsaPAL62* were analyzed using online bioinformatic tools from NCBI and ExPASy. Open reading frame (ORF) finding was performed using the on-line program (http://www.ncbi.nlm.nih.gov/gorf/orfig.cgi). Various physicochemical parameters of proteins were evaluated using the ProtParam tool (http://web.expasy.org/protparam/). TMHMM (http://www.cbs.dtu.dk/services/TMHMM/) was used to predict the transmembrane helices of proteins, and SignalP 4.1 (http://www.cbs.dtu.dk/services/SignalP/) was used to predict cleavage sites of signal peptides. Protein subcellular locations were predicted using TargetP 1.1 Server (http://www.cbs.dtu.dk/services/TargetP/), and functional sites of proteins were analyzed with PROSITE tools (http://prosite.expasy.org/). Concord (http://helios.princeton.edu/CONCORD/)[40] was used to predict the secondary structures of OsaPAL2 and OsaPAL62, and protein multiple sequence alignment was performed using ClustalX (version 2.1).[41] A phylogenetic tree was constructed using the neighbor-joining method with the MEGA5.1 program.[42]

2.6. Protein expression

The prokaryotic expression vector pET-28a (+) was digested with restriction endonucleases *Bam*HI and *Eco*RI to generate the linearized vector. Plasmids pEASY-OsaPAL2 and pEASY-OsaPAL62 were used as templates for sub-cloning the full-length sequences of OsaPALs with respective specific primer pairs (Table 1). After gel purification, the PCR product was sub-cloned into pET-28a (+) according to the In-Fusion® HD Cloning Kit protocol. Finally, sequencing was used to verify the integrity of plasmids pET28a–OsaPAL2 and pET28a–OsaPAL62 with both of them containing a His_6 tag.

The expression plasmids pET28a–OsaPAL2 and pET28a–OsaPAL62 were transformed into the expression host strain *Transetta* (DE3) grown in LB agar containing 170 μg ml^{-1} chloromycetin and 50 μg ml^{-1} kanamycin. After overnight incubation at 37 °C, a single clone of each was used to inoculate 20 ml of LB/chloromycetin/kanamycin at 37 °C, which was shaken at 200 rpm until the OD at 600 nm reached a value of 1.0, diluted 1 : 50 into 50 ml TB supplemented with 170 μg ml^{-1} chloromycetin and 50 μg ml^{-1} kanamycin, and then shaken at 200 rpm at 37 °C until the OD at 600 nm reached 0.8. Subsequently, 0.1 mM IPTG was added and after shaking at 150 rpm at 20 °C overnight, the induced cells were harvested by centrifugation (7500*g*, 2 min) at 4 °C. The pellets were then either stored at −80 °C or used directly.

2.7. Enzyme purification

For enzyme purification, all steps were performed at 4 °C. First, *E. coli* cells were washed and re-suspended in lysis buffer (pH 8.0, 20 mM sodium phosphate containing 5 mM imidazole and 300 mM NaCl). Cells were then lysed with a high-pressure homogenizer (800 bar, 3 passes), after which 1 U per ml DNaseI was added, and then the homogenate was incubated at 4 °C for approximately 2 h. After centrifugation at 10 000*g* for 15 min, the supernatant was passed through a 0.2 μm pore-size filter to remove *E. coli* cell debris and other contaminants, and then

Table 2 Oligonucleotide primer pairs used for site-directed mutagenesis in this study. The bases underlined in each primer are the codons introduced

Mutant	Template	Primer	Sequence
OsaPAL2F134H	pET28a–OsaPAL2	PAL2F134HF	5′-TGCAGAGAGAGTTGATAAGGCATCTGAATGCCGG-3′
		PAL2F134HR	5′-ATGCCTTATCAACTCTCTCTGCAGGGCGCCCCC-3′
OsaPAL2T196S	pET28a–OsaPAL2	PAL2T196SF	5′-TACGAGGCACCATCAGCGCCTCCGG-3′
		PAL2T196SR	5′-GCTGATGGTGCCTCGTAGAGGAAGGCA-3′
OsaPAL2V202S	pET28a–OsaPAL2	PAL2V202SF	5′-GCCTCCGGCGACCTAAGCCCCTTGTCCT-3′
		PAL2V202SR	5′-GCTTAGGTCGCCGGAGGCGGTGATGGTG-3′
OsaPAL2G209A	pET28a–OsaPAL2	PAL2G209AF	5′-TTGTCCTACATTGCCGCGCTTCTCACCG-3′
		PAL2G209AR	5′-CGCGGCAATGTAGGACAAGGGGACTAGG-3′
OsaPAL2V202S/G209A	pET28a–OsaPAL2	PAL2G209AF	5′-TTGTCCTACATTGCCGCGCTTCTCACCG-3′
		PAL2DMR	5′-CGCGGCAATGTAGGACAAGGGGCTTAGG-3′
OsaPAL2T196S/V202S/G209A	pET28a–OsaPAL2V202S/G209A	PAL2T196SF	5′-TACGAGGCACCATCAGCGCCTCCGG-3′
		PAL2T196SR	5′-GCTGATGGTGCCTCGTAGAGGAAGGCA-3′
OsaPAL62F128H	pET28a–OsaPAL62	PAL62F128HF	5′-TTCAGAAGGAGCTCATCAGACATCTCAACGCGGG-3′
		PAL62F128HR	5′-ATGTCTGATGAGCTCCTTCTGAAGGGCACCACC-3′
OsaPAL62T194S	pET28a–OsaPAL62	PAL62T194SF	5′-CTCCGCGGCACGATCAGCGCCTCCGGCG-3′
		PAL62T194SR	5′-GCTGATCGTGCCGCGGAGAGGGAGGCAC-3′
OsaPAL62V200S	pET28a–OsaPAL62	PAL62V200SF	5′-GCCTCCGGCGACCTCAGCCCGTTGTCCT-3′
		PAL62V200SR	5′-GCTGAGGTCGCCGGAGGCGGTGATCGTG-3′
OsaPAL62G207A	pET28a–OsaPAL62	PAL62G207AF	5′-ATATCGCCGCGATCCTCACCG-3′
		PAL62G207AR	5′-CGCGGCGATATAGGACAACGG-3′
OsaPAL62V200S/G207A	pET28a–OsaPAL62	PAL62DMF	5′-TTGTCCTATATCGCCGCGATCCTCACCG-3′
		PAL62DMR	5′-CGCGGCGATATAGGACAACGGGCTGAGG-3′
OsaPAL62T194S/V200S/G207A	pET28a–OsaPAL62V200S/G207A	PAL62T194SF	5′-CTCCGCGGCACGATCAGCGCCTCCGGCG-3′
		PAL62T194SR	5′-GCTGATCGTGCCGCGGAGAGGGAGGCAC-3′

loaded onto a pre-equilibrated column containing Ni-NTA resin. The column was washed with washing buffers (pH 8.0, 20 mM sodium phosphate buffer containing 20–50 mM imidazole and 300 mM NaCl) to remove non-specifically bound proteins, after which an elution buffer (pH 8.0, 20 mM sodium phosphate containing 300 mM imidazole and 300 mM NaCl) was used to elute the His_6-tagged protein.

To remove small molecules such as imidazole, dialysis was performed. A semipermeable membrane with a molecular weight cutoff of 30 kDa was selected and approximately 20 ml protein sample was dialyzed against 1 l dialysis buffer (pH 8.0, 10 mM sodium phosphate) for 4 h at 4 °C with four changes of dialysis buffer. Proteins were then dried in a vacuum freeze-dryer and stored at −80 °C until use.

2.8. Enzyme activity and analysis

Enzyme activity of recombinant purified OsaPALs was unambiguously determined by a combination of HPLC-UV, HPLC-MS and ^1H and ^{13}C NMR spectroscopies using L-Phe and L-Tyr as substrates. The reaction mixture (200 μl), containing 0.1 M CHES buffer (pH 9.5), 100 mM L-Phe or 10 mM L-Tyr and different amounts of purified protein, was incubated at 37 °C for 30 min, and then terminated by adding 200 μl chloroform. After centrifugation at 15 000*g* for 10 min, the supernatant was filtered through an 0.2 μm pore-size filter and analyzed by HPLC-UV on a HITACHI LaCrom elite L-2000 HPLC system (HITACHI, Toyokawa, Japan) using a C18 column [YMC-Pack ODS-A (5 μm, 12 nm, 250 × 4.6 mm)] and gradient elution using 0.05% aqueous trifluoroacetic acid (solvent A) and CH_3CN (solvent B). After pre-equilibration in 98 : 2 A : B (v/v), the sample was injected and chromatographed using a linear gradient to 35 : 65 A : B (v/v) over 26 min at a flow rate of 1 ml min^{-1}.

The reaction products of L-Phe (or L-Tyr), catalyzed by OsaPAL2 and OsaPAL62 [named OsaPAL2-L-Phe-*p* (or OsaPAL2-L-Tyr-*p*) and OsaPAL62-L-Phe-*p* (or OsaPAL62-L-Tyr-*p*), respectively], were isolated using a YMC semi-preparative column [YMC-Pack ODS-A (5 μm, 12 nm, 250 × 10 mm)] using a linear gradient elution from 40–65% solvent B in 15 min for L-Tyr products and a linear gradient elution from 40–80% solvent B in 15 min for L-Phe products, both of them at a flow rate of 2 ml min^{-1}. UV detection at 275 and 310 nm was used for enzymatic products of L-Phe and L-Tyr, respectively. HPLC-MS was performed using an Agilent 1200 RRLC series HPLC system (Agilent Technologies, Waldbronn, Germany) coupled with a QTRAP tandem mass spectrometer (QTRAP 2000, Applied Biosystems/MDS SCIEX) equipped with a Turbo Ion spray source (Concord, ON, Canada) operated in the negative ionization mode and controlled by Analyst 1.5 software. Mass spectra were obtained in the enhanced full mass scan mode in the range of *m*/*z* 100–1000. NMR spectra of products dissolved in deuterated dimethyl sulfoxide (DMSO-d6) and placed in 5 mm NMR tubes were recorded using Bruker AVIII-600 and Bruker AVIII-500 NMR spectrometers (Bruker-Biospin, Germany), which were operated at 600 and 500 MHz, respectively. Chemical shifts (δ) and coupling constants (*J*) were provided in ppm and hertz (Hz), respectively.

2.9. Optimum pH of recombinant OsaPALs

To evaluate the effect of pH on enzyme activity, the following buffers were used: 0.1 M MES, pH 5.5–6.7; 0.1 M HEPES, pH 6.8–8.2; 0.1 M CHES, pH 8.6–10.0; 0.1 M CAPS, pH 9.7–11.1; and 0.1 M Na_2HPO_4–NaOH, pH 11.5–12.0. Assays were performed at a constant temperature of 37 °C for 20 min and monitored continuously with a multimode reader. Controls without enzymes were included and each experiment was performed in triplicate.

2.10. Optimum temperature of recombinant OsaPALs

For determination of the optimal temperature, reactions were performed in 0.1 M CHES buffer (pH 9.5) and pre-incubated at different temperatures in the range 30–60 °C for 10 min. Substrates were added to initiate the reactions, and, after incubation for 15 min, during which time the change in absorption was measured, glacial acetic acid was added to terminate the reaction. Controls without enzymes were included and each experiment was performed in triplicate.

2.11. Kinetic analysis of recombinant OsaPALs

Kinetic analysis of native enzymes was performed at pH 9.5 and 44 °C using a total volume of 200 μl, which contains various concentration ranges of substrates (L-Phe 9.76 μM to 20 mM; L-Tyr 15.6 μM to 8 mM) and purified proteins (for L-Phe: 6.3 μg OsaPAL2, 15.5 μg OsaPAL62, 47.32 μg OsaPAL2F134H, 36.5 μg OsaPAL62F128H, 19.6 μg OsaPAL2T196S, 22.8 μg OsaPAL62T194S, 23 μg OsaPAL2V202S, 647.2 μg OsaPAL62V200S, 8.8 μg OsaPAL2G209A, 12.1 μg OsaPAL62G207A; For L-Tyr: 135.6 μg OsaPAL2, 136.4 μg OsaPAL62, 236.6 μg OsaPAL2F134H, 182.84 μg OsaPAL62F128H, 175.2 μg OsaPAL2G209A, 120.6 μg OsaPAL62G207A). Assays for individual substrates were performed in triplicate for 10 min (L-Phe) or 20 min (L-Tyr). The formation of product was continuously monitored with a multimode reader. Kinetic constants values were determined from Lineweaver–Burk plots. All kinetic assays were performed in triplicate and controls without enzymes or substrates were included.

2.12. Site-directed mutagenesis

Site-directed mutagenesis was used to investigate the importance of various amino acid residues in determining enzyme activity. Point and double mutations were introduced into OsaPALs by PCR-based amplification of the entire OsaPAL expression plasmid (pET28a–OsaPAL2 or pET28a–OsaPAL62) using two mutated oligonucleotide primers (Table 2), each complementary to the opposite strand of the vector. All components necessary for PCR-based mutagenesis were provided in the Fast Mutagenesis System kit and were used according to the manufacturer's instructions. All mutants were confirmed by sequencing and those plasmids with target substitutions and without other unwanted mutations were retained. Triple mutations were introduced in the same way using already existing mutants as templates.

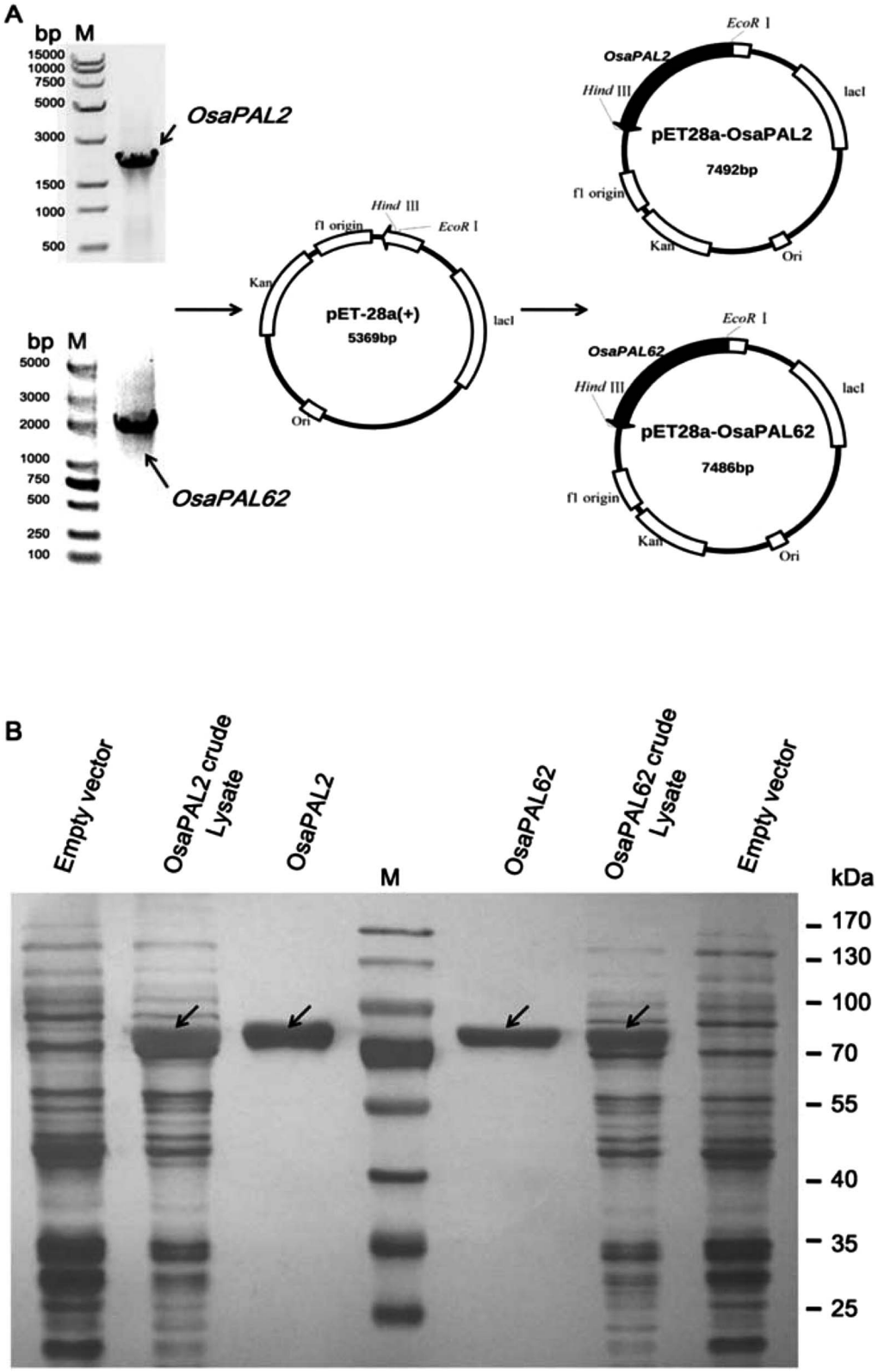

Fig. 2 cDNA cloning and wild-type enzyme expression. (A) cDNA cloning of *OsaPAL2* and *OsaPAL62* and the construction of expression plasmids. (B) SDS-PAGE analysis of recombinant wild-type enzymes. From right to left: empty vector as the control, OsaPAL2 crude lysate, purified wild-type OsaPAL2, protein standards, purified wild-type OsaPAL62, OsaPAL62 crude lysate, empty vector and molecular weights corresponding to protein standards. The arrows indicate the target proteins.

2.13. Comparison of mutant activities

To compare the activities of wild-type and mutants, mutants were expressed and purified according to the methods described above. The purity of proteins was estimated by SDS-PAGE and pure proteins were dried in a vacuum freeze-dryer and stored at −80 °C. Prior to use, enzymes were dissolved in CHES buffer (0.1 M, pH 9.5), and the proteins were determined using the Bio-Rad protein assay (Bio-Rad, USA). HPLC was used to compare the catalytic activities of different mutants. Assays were performed in 1000 μl aqueous buffer containing 100 mM CHES (pH 9.5) and 25 μg enzyme. After pre-incubation at 37 °C for 10 min, substrates (50 mM L-Phe or 10 mM L-Tyr) were added and reactions run for 1, 2 or 3 h before being terminated by boiling for 5 min. Mixtures were then centrifuged (15 000*g*, 10 min) and 15 μl injected into the HPLC system. Each assay was performed in triplicate. Kinetic constants of some single mutants were also determined using the above procedure.

3. Results and discussion

3.1. Transcriptome analysis of OsaPAL homology

OSW-1 is a cholestane saponin featuring a novel 3β,16β,17α-trihydroxycholest-5-en-22-one aglycone with an acylated disaccharide attached to the 16-hydroxyl group (Fig. 1A). Biogenetic analysis showed that there were at least six kinds of enzymes responsible for OSW-1 biosynthesis, including terpenoid biosynthetic enzymes and steroid pathway enzymes, resulting in OSW-1 aglycone formation. Moreover, cytochrome P450 hydroxylase is able to add hydroxyl groups to the C-3, 16 and 17 positions of OSW-1 aglycone, and glycosyltransferase is involved in disaccharide moiety attachment to 16-OH of OSW-1 aglycone. Note that acyltransferases catalyze the introduction of the acetyl and the 4-methoxybenzoyl groups on the disaccharide moiety, while enzymes involved in nucleotide sugar donors biosynthesis provide glycosyl donors in glycosylation reactions and phenylpropanoid biosynthetic pathway enzymes convert aromatic amino acids to 4-methoxybenzoyl group (Fig. 1A). A total of more than 40 enzymes were deduced to be involved in the biosynthesis of OSW-1. It will take much more time to isolate and further characterize the function of all these genes using conventional molecular biology technologies. Thus, it is particularly important to apply a high-throughput method, which allows for drastically quicker and cheaper gene discovery and leads towards a far more comprehensive view of the OSW-1 biosynthetic pathway. The advent of next-generation sequencing approaches such as transcriptomic analysis provides a platform that has been proven to be critical in speeding up of the identification of a large number of related genes of secondary products. In the previous investigation, about 40 contigs and unigenes were retrieved and identified to be responsible for phenylpropanoid biosynthetic pathway from transcriptome sequence data of *O. saundersiae*.[39] Furthermore, batch alignment results revealed that there are four unigenes showing high similarities with PALs. These four unigenes, namely, 25029, 25031, 26221 and 26880, were 2150, 2130, 1409, and 317 bp in length, respectively. A batch BlastX search of the GenBank with the four unigenes indicated that none of these unigenes contained a full-length CDS. Of them, unigenes 26880 and 25029 had the equal sequence identity with the same PALs deposited in GenBank, suggesting that they were situated within the same candidate PAL. It is the same case with unigene 26221 and 25031. Furthermore, sequence alignment analysis postulated that unigenes 26880 and 25029 were the 5′- and 3′-end of one candidate PAL, while unigenes 26221 and 25031 were the 5′ and 3′-end of another candidate PAL, respectively. Accordingly, a gene family containing two PAL cDNAs was acquired by transcriptomic analysis.

3.2. Cloning and analysis of the full-length cDNAs encoding OsaPALs

Two full-length members of the *PAL* gene family were isolated from *O. saundersiae* by nested PCR using gene-specific primers (Fig. 2A and Table 1). Identity between the cDNA sequences and the results of transcriptome sequencing, which were verified by sequencing, indicated the presence of a *bona fide PAL* gene family in plants. Sequence information for the two cDNAs, designated *OsaPAL2* and *OsaPAL62*, was deposited in the GenBank database (*OsaPAL2* accession number KF741222; *OsaPAL62* accession number KF741223). *OsaPAL2* was derived from the unigenes 26221 and 25031 and contained an ORF of 2136 bp. *OsaPAL62* overlapped with unigenes 26880 and 25029 at the 5′ and 3′ ends, respectively, and it was 2130 bp in length. Sequencing identification proved the two cDNAs to be *bona fide PALs* of *O. saundersiae*, which is consistent with the fact that PALs are encoded by gene families in plant species such as *Rubus idaeus*,[43] *Arabidopsis*[44] and *Populus trichocarpa*.[45] Moreover, due to a lack of the genome sequence, we could not determine if the two cDNAs were derived from alternative splicing.

The proteins encoded by *OsaPAL2* and *OsaPAL62* were predicted by ProtParam tool to be polypeptides containing 711 and 709 amino acids with molecular weights of 77 103.9 and 76 570.6 Da, respectively. The instability indices (II) indicated that the two proteins were stable (II < 40), and their low grand average of hydropathicity (GRAVY) values of −0.139 (OsaPAL2) and −0.112 (OsaPAL62) indicate their hydrophobicity.[46] The theoretical pI values of 5.64 (OsaPAL2) and 6.15 (OsaPAL62) were <7, revealing their acidic nature. The TMHMM tool indicated that OsaPAL2 or OsaPAL62 are not transmembrane proteins, and SignalP 4.1 showed no signal peptide or signal peptide cleavage sites, indicating that they are not secreted proteins. These results are consistent with the predictions of TargetP 1.1 that the two proteins are not located in chloroplasts, mitochondria or secretory pathways.

According to the results provided by PROSITE tools, both OsaPALs contain a 17-amino acid motif (GTITASGDLVPLSYIAG), which is a conserved signature in the superfamily of ammonia lyases, including PAL, tyrosine ammonia lyase (TAL, EC 4.3.1.23) and histidine ammonia lyase (HAL, EC 4.3.1.3). The motif contains an active Ala–Ser–Gly (A–S–G) triad, which can autocatalytically be converted into a MIO (4-methylidene-imidazole-5-one) ring that serves as a prosthetic group and activates

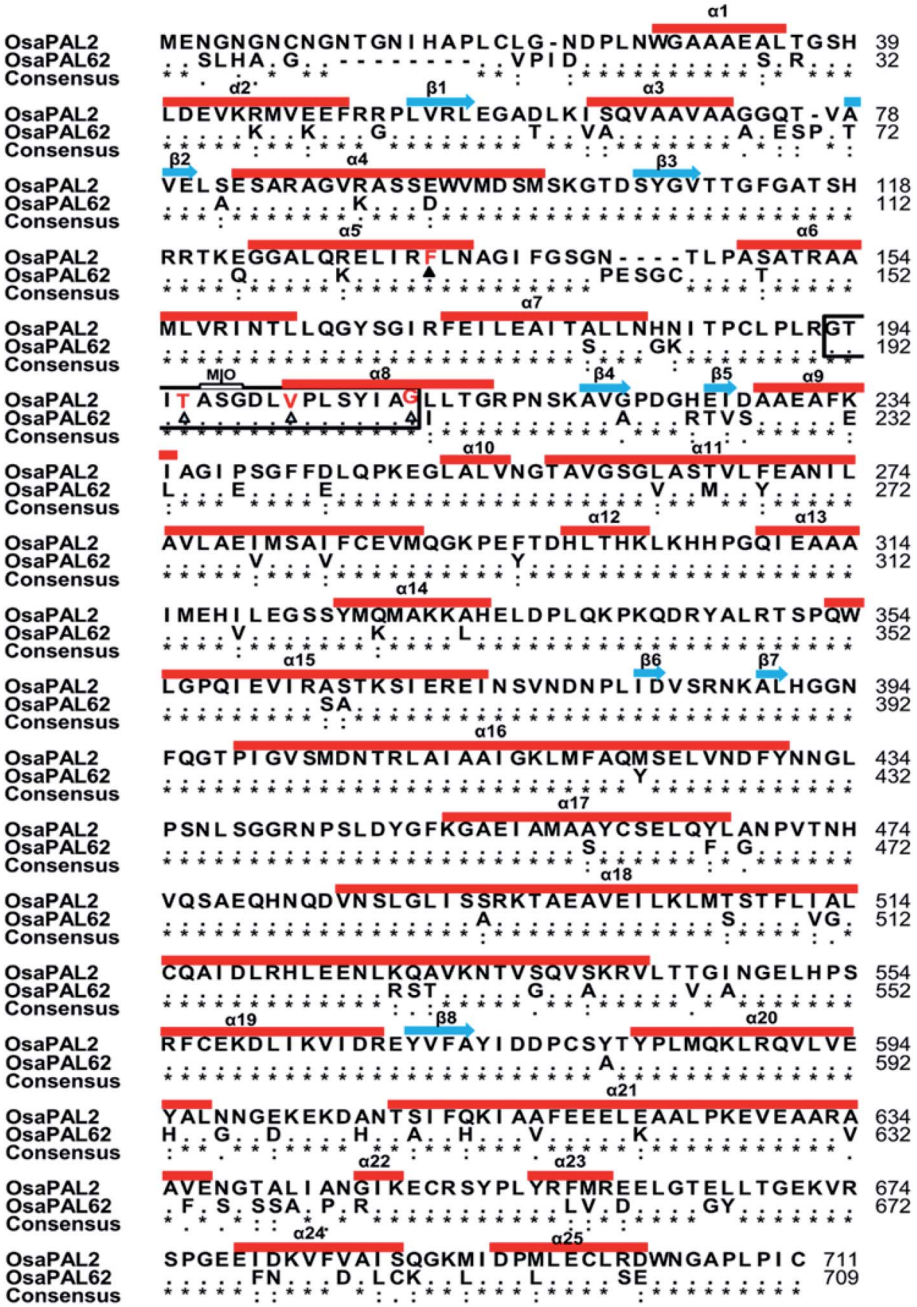

Fig. 3 Amino acid sequence alignment of OsaPAL2 and OsaPAL62. Asterisks, dots and colons indicate identical, semi-conserved and conserved substitutions, respectively. The open and filled triangles indicate the residues individually substituted in this study; moreover, the filled triangles indicate the positions of residues believed to be responsible for substrate selectivity. Rectangles and arrows represent the predicted α-helices and β-strands, respectively. The highly conserved phenylalanine ammonia lyase signature is circled and the conserved active site motif (A–S–G) is indicated by the bracket.

substrates by means of electrophilic interactions.[47–49] With respect to the predicted secondary structure, both proteins had 8 β-sheets and 25 α-helices with the residues differing between the two proteins found primarily in random coils (Fig. 3).

3.3. Multiple sequence alignment and phylogenetic analysis

BlastP in NCBI (http://www.ncbi.nlmnih.gov/BLAST) and multi-alignment analysis according to CLUSTAL X algorithm indicate that the deduced polypeptide of OsaPAL2 is highly homologous to that of MbPAL (BAG70992.1) in *Musa balbisiana*. OsaPAL62 is highly homologous to PALs of some species, *e.g.*, it shares 85% homology with the PAL sequence of *Cinnamomum osmophloeum* CoPAL (AFG26322.1), while the OsaPAL2 and OsaPAL62 sequences are 83.6% homologous.

Phylogenetic analysis revealed that the PALs of angiosperm plants are divided into two clusters: those from dicotyledonous

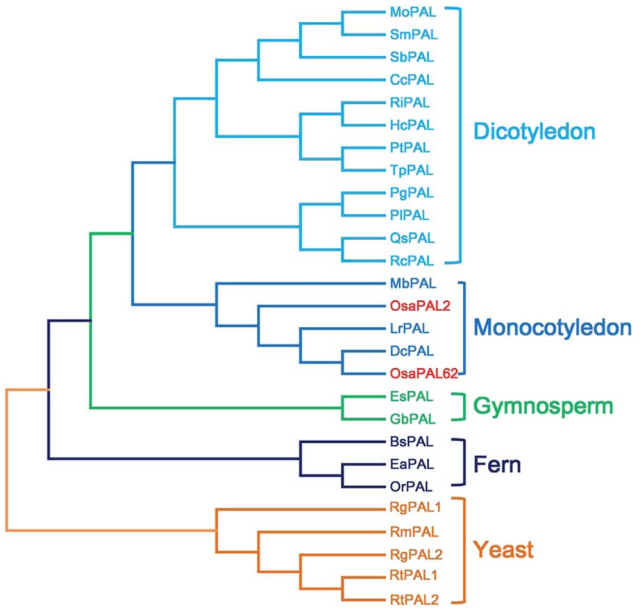

Fig. 4 Phylogenetic analysis of OsaPAL2, OsaPAL62 and other PALs. The phylogenetic tree was constructed using the neighbor-joining method available in the MEGA5.1 program. It shows a comparison of the sequences from the dicotyledons: *Paeonia lactiflora* PlPAL (AFI71896.1), *Rhus chinensis* RcPAL (AGH13333.1), *Populus trichocarpa* PtPAL (ACC63887.1), *Hibiscus cannabinus* HcPAL (AFN85669.1), *Trifolium pratense* TpPAL (AAZ29733.1), *Scutellaria baicalensis* SbPAL (ADN32768.1), *Melissa officinalis* MoPAL (CBJ23826.1), *Salvia miltiorrhiza* SmPAL (ABD73282.1), *Quercus suber* QsPAL (AAR31107.1), *Rubus idaeus* RiPAL (AAF40224.1), *Platycodon grandiflorus* PgPAL (AEM63671.1) and *Coffea canephora* CcPAL (AEO92028.1); monocotyledons: *Musa balbisiana* MbPAL (BAG70992.1), *Lycoris radiate* LrPAL (ACM61988.1) and *Dendrobium candidum* DcPAL (AGC23439.1); gymnosperms: *Ginkgo biloba* GbPAL (ABU49842.1) and *Ephedra sinica* EsPAL (BAG74772.1); the ferns: *Blechnum spicant* BsPAL (AAW80643.1), *Equisetum arvense* EaPAL (AAW80639.1) and *Ophioglossum reticulatum* OrPAL (AAW80642.1); and yeasts: *Rhodotorula mucilaginosa* RmPAL (CAA31486.1), *Rhodosporidium toruloides* RtPAL2 (AAA33883.1), *Rhodotorula glutinis* ATCC 204091 RgPAL2 (EGU13302.1), *Rhodotorula glutinis* RgPAL1 (ABB04148.1) and *Rhodosporidium toruloides* RtPAL1 (CAA35886.1).

plants [*e.g.* PlPAL (AFI71896.1) from *Paeonia lactiflora* and RcPAL (AGH13333.1) from *Rhus chinensis*] and those from monocotyledon plants [*e.g.* MbPAL (BAG70992.1) from *Musa balbisiana*] (Fig. 4). Amino acid sequences of OsaPAL2 and OsaPAL62 belong to the latter cluster. It has been reported that PALs from monocotyledons always possess TAL activity,[50,51] suggesting that OsaPAL2 and OsaPAL62 may have PAL/TAL activities. In the resulting phylogeny, OsaPAL62 and PALs from *Lycoris radiate* (LrPAL) and *Dendrobium candidum* (DcPAL) were clustered in the same clade, whereas OsaPAL2 was alone in a neighboring branch, suggesting that it belongs to a different subfamily. In addition, PALs of ferns and gymnosperms formed independent clusters, a result consistent with the evolution of plants. PALs of plants and yeasts have a common ancestor but are separated by a large evolutionary distance with only 36% homology between OsaPAL2 and RmPAL (CAA31486.1) from *Rhodotorula mucilaginosa*.

3.4. Expression of recombinant proteins and catalytic product analysis

The two ORFs were sub-cloned into *E. coli* vector pET-28a (+) by the In-Fusion method, which resulted in the heterologous plasmids pET28a–OsaPAL2 and pET28a–OsaPAL62 (Fig. 2A). Recombinant His_6-tagged OsaPAL2 and OsaPAL62 were expressed in *E. coli* and purified on Ni-NTA resin. SDS-PAGE analysis showed that both OsaPAL2 and OsaPAL62 were expressed and had molecular weights of approximately 75 kDa (Fig. 2B).

Enzymes were incubated with L-Phe or L-Tyr, and the products were analyzed by HPLC-UV, HPLC-MS, and NMR. The data showed that the products of L-Phe catalyzed by OsaPAL2 and OsaPAL62 (OsaPAL2-L-Phe-*p* and OsaPAL62-L-Phe-*p*, respectively) had the same UV spectra as that of *trans*-cinnamic acid. In HPLC-MS, the most intense peaks of the two products were located at *m*/*z* 147 due to the loss of a hydrogen radical. The structure of these two products was further confirmed by NMR after semi-preparative isolation to be *trans*-cinnamic acid (Fig. 5).

For the corresponding products of L-Tyr, HPLC-UV analysis showed that both enzymes converted L-Tyr to the new products, OsaPAL2-L-Tyr-*p* and OsaPAL62-L-Tyr-*p*, which exhibit the same UV-spectra as that of *p*-coumaric acid. Both OsaPAL2-L-Tyr-*p* and OsaPAL62-L-Tyr-*p* exhibited an abundant ion at *m*/*z* 163 due to the loss of a hydrogen atom with subsequent loss of a carboxyl group to form an ion at *m*/*z* 119. NMR analysis further confirmed OsaPAL2-L-Tyr-*p* and OsaPAL62-L-Tyr-*p* to be *p*-coumaric acid (Fig. 6).

These results strongly suggest that OsaPAL2 and OsaPAL62 have both PAL and TAL activity, consistent with the activity of PALs present in other monocotyledonous plants such as *Zea mays*[51] and *Phyllostachys edulis*.[52]

3.5. Biochemical analysis of OsaPALs

In many previous studies, the formation of *trans*-cinnamic acid was usually monitored at 275 or 280 nm.[26,51,53] However, at this wavelength, the substrate L-Phe shows UV absorption (Fig. 5); thus, the determination of *trans*-cinnamic acid will be disturbed when using a multimode reader. Therefore, to eliminate the effect of the substrate, we monitored absorbance at 300 nm.

The optimal pH and temperature for efficient enzyme activity of purified enzymes, OsaPAL2 and OsaPAL62, were found to be similar to those for L-Phe and L-Tyr deamination (Fig. 7). Both enzymes functioned better in the pH range of 8.5–10.0 and showed only low activity at pH <7.0 or >11.0. This optimum pH range is comparable to that of PALs isolated from other monocotyledonous species such as PePAL from *Phyllostachys edulis* (pH 8.5–9.0),[52] SmPAL1 from *Salvia miltiorrhiza* (pH 8.7)[2] and BoPAL4 from *Bambusa oldhamii* (pH 9.0).[50] The effect of temperature on the activity of OsaPAL2 and OsaPAL62 was similar with both showing highest activity at 44 °C. Similar temperatures have been observed for maximum activity of PALs in *Rhus chinensis* (45 °C)[1] and *Arabidopsis* (46–48 °C)[44] with a slightly lower temperature being optimum for AvPAL in

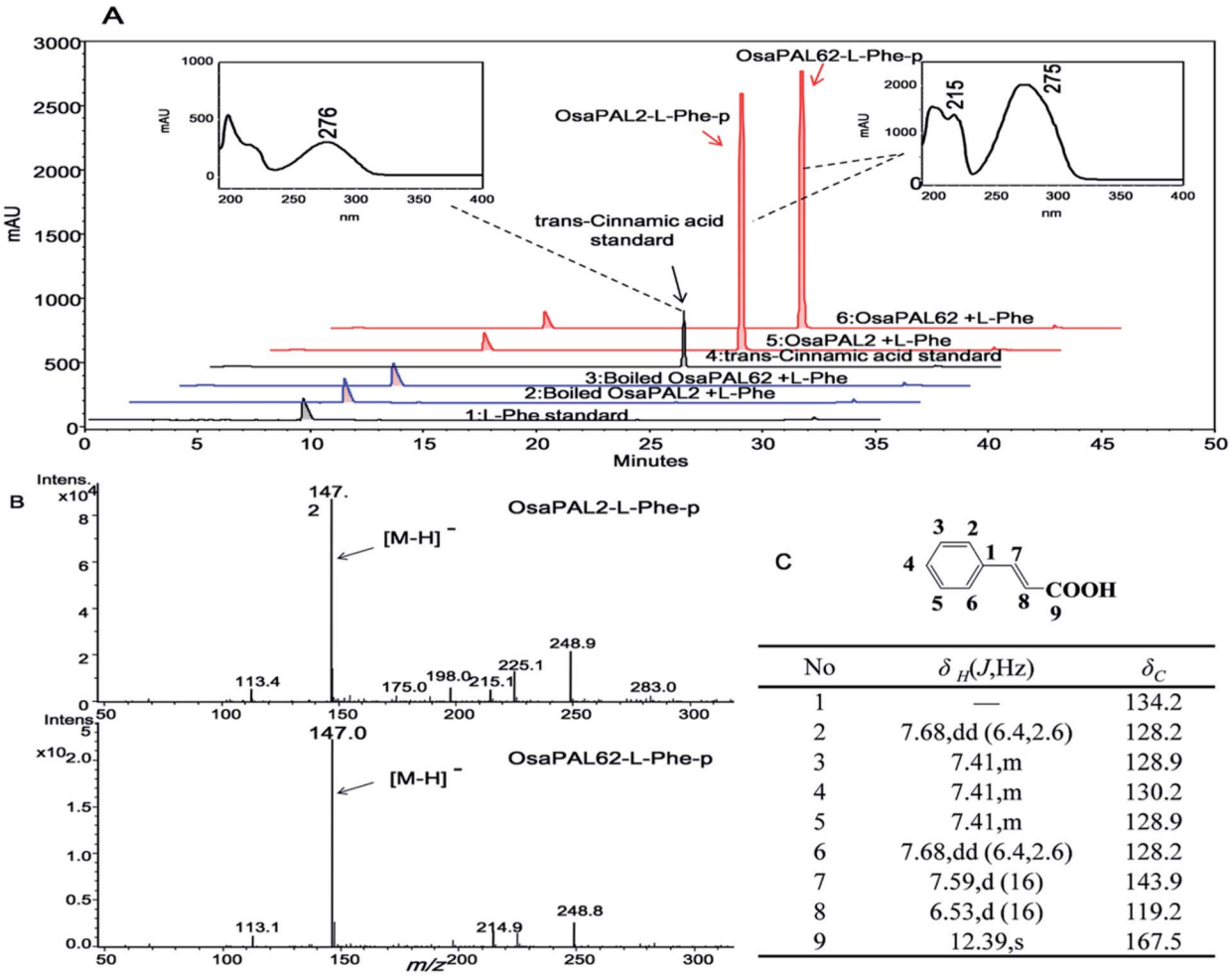

No	δ_H(J,Hz)	δ_C
1	—	134.2
2	7.68,dd (6.4,2.6)	128.2
3	7.41,m	128.9
4	7.41,m	130.2
5	7.41,m	128.9
6	7.68,dd (6.4,2.6)	128.2
7	7.59,d (16)	143.9
8	6.53,d (16)	119.2
9	12.39,s	167.5

Fig. 5 Analysis of the products of OsaPALs *in vitro* assays with L-Phe. (A) HPLC analysis: traces 1 and 4 show the substrate (L-Phe) and product (*trans*-cinnamic acid) standard, respectively; traces 2 and 3 are the controls showing the results for boiled enzymes incubated with the substrate (L-Phe); traces 5 and 6 are the results for purified wild-type enzymes incubated with L-Phe and the resulting products have similar UV-spectra with *trans*-cinnamic acid. (B) Mass spectra (MS) analysis: both OsaPAL2-L-Phe-*p* and OsaPAL62-L-Phe-*p* exhibit strongest ion peaks at 147 *m*/*z*. (C) NMR analysis results indicate that OsaPAL2-L-Phe-*p* and OsaPAL62-L-Phe-*p* have the same structure.

A. variabilis (40 °C)[26] and a higher temperature being optimum for Pal in *Helianthus annuus* L. (55 °C).[54]

Assays were performed with L-Phe or L-Tyr as the substrate at an optimum pH and temperature to evaluate the kinetic constants of OsaPAL2 and OsaPAL62 (Fig. 7,8 and Table 3). Both wild-type enzymes displayed marked kinetic preference for L-Phe as K_m of OsaPAL2 for L-Phe (371.5 ± 26.7 μM) was about 30-fold lower than that for L-Tyr (11690 ± 1410 μM) and k_{cat}/K_m for L-Phe (2160 M^{-1} s^{-1}) was substantially higher than that for L-Tyr (39.65 M^{-1} s^{-1}). A similar situation was found as a K_m of OsaPAL62 for L-Phe (593.1 ± 48.6 μM) was about 60-fold lower than that for L-Tyr (39 280 ± 472 μM) and k_{cat}/K_m for L-Phe (934.9 M^{-1} s^{-1}) was higher than that for L-Tyr (16.69 M^{-1} s^{-1}). Assays performed to determine the kinetic constants of OsaPAL2 and OsaPAL62 for L-Tyr were unable to saturate the enzymes due to the lower appetency and solubility limitations of L-Tyr.[44] The K_m values of these enzymes for L-Phe were similar to those of other PALs such as the PAL of *Oryza sativa* (500 μM)[55] and the BoPAL2 of *B. oldhamii* (333 μM).[50] The k_{cat}/K_m values of these two wild-type enzymes for L-Phe were lower than those of the PALs in *Zea mays* (3.9×10^4 M^{-1} s^{-1})[51] and *Jatropha curcas* L. (1.384×10^4 M^{-1} s^{-1}).[56]

The higher L-Phe and lower L-Tyr deamination activity of OsaPAL2 and OsaPAL62 is consistent with previous studies on PALs found in monocotyledons.[51] Moreover, the OsaPALs were able to catalyze the reversible reaction whereby *trans*-cinnamic acid is converted to L-Phe, an ability that was also observed with some other PALs (data not shown).

3.6. Identification of specificity determining residues

OsaPAL2 and OsaPAL62 also have TAL activity, allowing direct conversion of L-Tyr to *p*-coumarate, and thus eliminating the requirement for the hydroxylation step. This activity is valuable for designing heterologous pathways for producing target metabolites. One underlying mechanism of bi-functional PAL is based on the presence of a Phe residue controlling the substrate selection.[57] Although several experiments have supported this

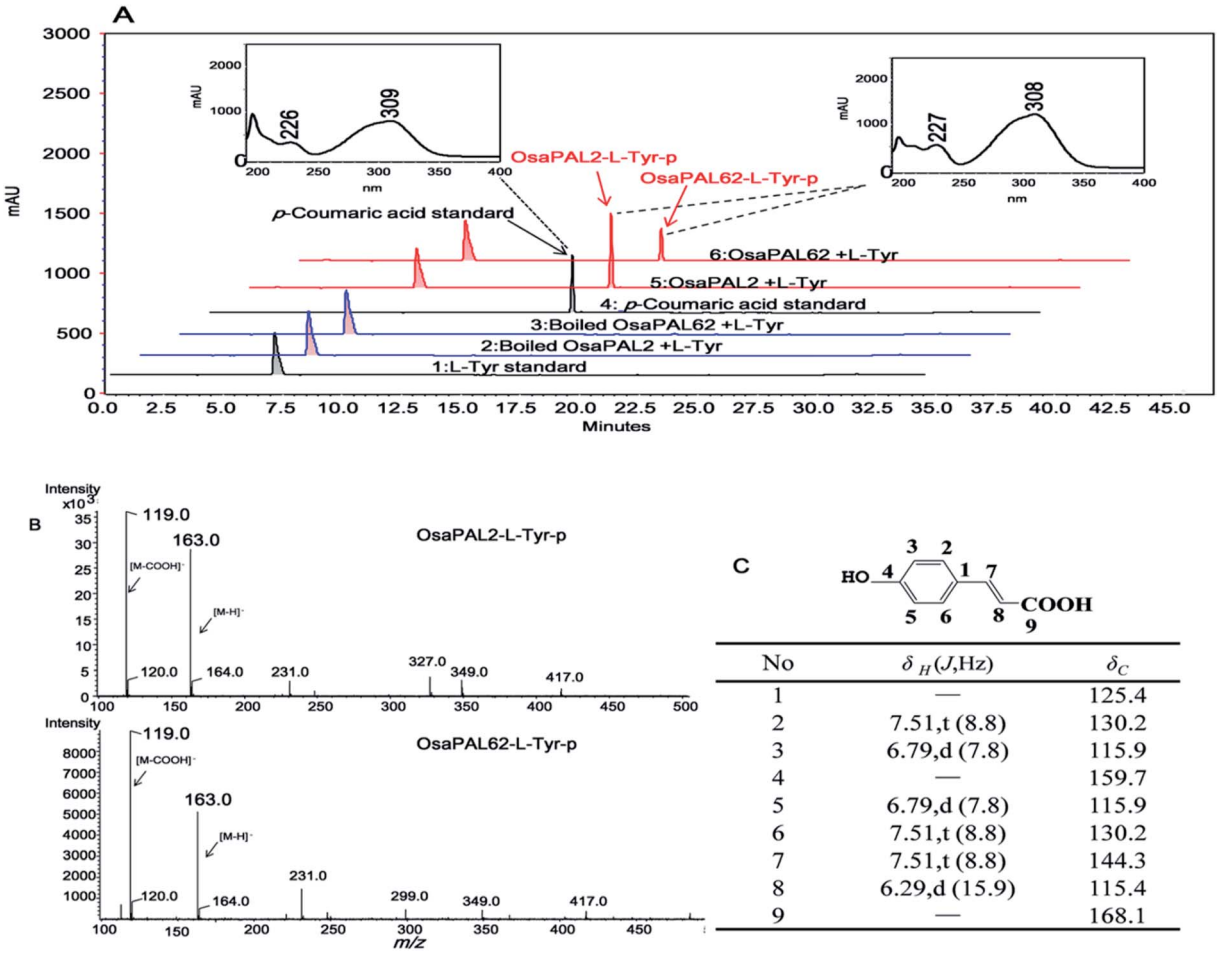

Fig. 6 Analysis of the products of OsaPALs *in vitro* assays with L-Tyr. (A) HPLC analysis: traces 1 and 4 show the substrate (L-Tyr) and product (*p*-coumaric acid) standard, respectively; traces 2 and 3 are the controls showing the results for boiled enzymes incubated with the substrate (L-Tyr); Traces 5 and 6 are the results of purified wild-type enzymes incubated with L-Tyr and the resulting products have similar UV-spectra with *p*-coumaric acid (note that the wavelength was set to 275 nm to visualize the substrate L-Tyr). (B) Mass spectra (MS) analysis: both OsaPAL2-L-Tyr-*p* and OsaPAL62-L-Tyr-*p* have the same peaks at *m*/*z* 163 and 119. (C) NMR analysis results and the structure of the product.

hypothesis, various questions remain unaddressed. In a report by Watts *et al.*,[57] when Phe144 residue was replaced by His in *A. thaliana* PAL1, the mutant displayed a marked reduction (80-fold) in k_{cat}/K_m value together with an 18-fold increase in catalytic efficiency towards tyrosine. This result clearly showed that Phe144 controlled substrate selection;[57] however, Hsieh *et al.*[50] did not obtain the same results. When Phe133 was substituted with His, only a slightly increased k_{cat}/K_m value toward tyrosine was observed in the F133H mutant. The authors inferred that other residues also contribute to the substrate selectivity of PALs. In view of this result, they proposed that further site-directed mutagenesis experiments would be necessary for elucidation of the underlying mechanism of substrate selectivity.[50] This situation poses the question of how exactly the Phe residue functions in the substrate selectivity switch. Site-directed mutagenesis of Phe residue was accordingly performed in OsaPALs with the aim of identifying this function.

TAL and PAL have different substrate specificities associated with a difference in a residue corresponding to F134 in OsaPAL2 and F128 in OsaPAL62 (Fig. 3). This residue gives rise to low L-Tyr deamination activity, which is improved by substituting the two residues with H to give OsaPAL2F134H and OsaPAL62F128H (Table 3, Fig. 8–10). The optimum pH and temperature for the two mutants are nearly the same as those of the wild-type proteins (ESI Fig. 1–3†). The kinetic parameters, however, varied markedly when F was mutated to H. For OsaPAL2F134H, the values of K_m and k_{cat}/K_m for L-Tyr were 16.9-fold lower and 7.0-fold higher, respectively, than those for the wild-type enzyme. After F → H mutation, the activity toward L-Phe decreased with K_m being 3-fold higher than that for OsaPAL2 and k_{cat}/K_m being reduced by 86% (Table 3). OsaPAL62F128H exhibited remarkable TAL activity compared with the wild-type enzyme (Table 3, Fig. 8 and 10) with values of K_m and k_{cat}/K_m for L-Tyr were approximately 30-fold lower and 6-fold higher, respectively, than those for the wild-type enzyme. The substitution of F with H resulted in a significantly reduced activity for L-Phe with lower affinity (K_m 2.8-fold higher than that of wild-type) and lower catalytic efficiency (k_{cat}/K_m 4.7-fold lower than that of the wild-type) (Table 3).

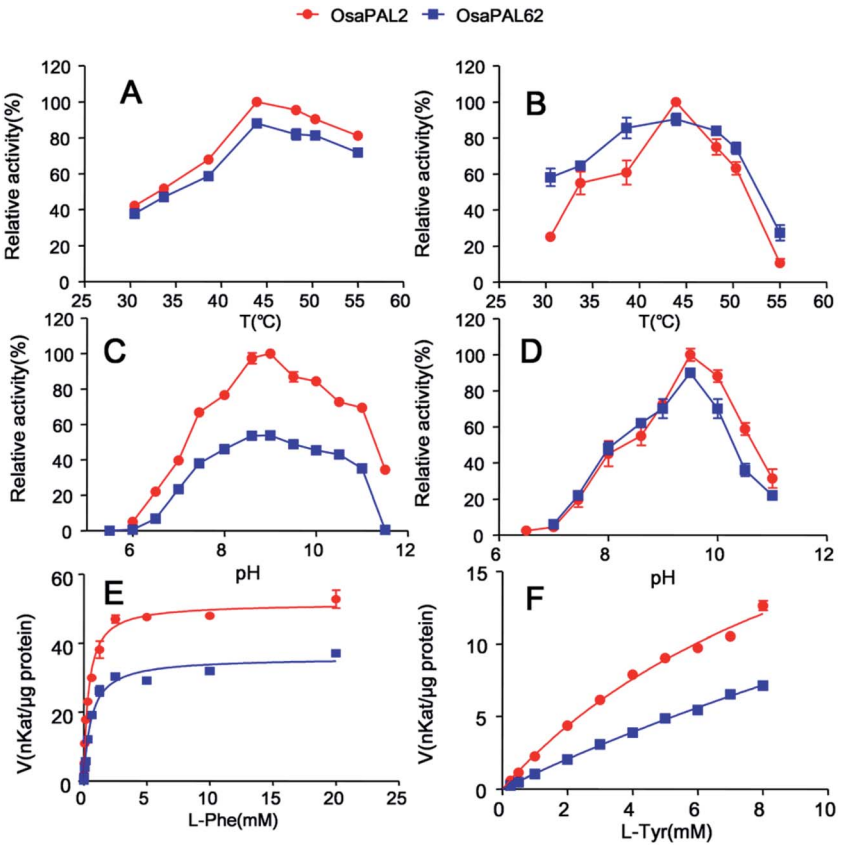

Fig. 7 Biochemical characterization and comparison of recombinant enzymes. The optimum temperatures and pH for catalyzing L-Phe (A and C) and L-Tyr (B and D) of both enzymes were determined. (E and F) are overlays of substrate saturation plots of the two enzymes using L-Phe and L-Tyr as substrates performed in CHES buffer (0.1 M, pH 9.5) at 44 °C by continuously monitoring changes in absorbance at 300 and 310 nm, respectively. (Note that at a wavelength of 275 nm, the substrate L-Phe shows UV absorption, which was eliminated by monitoring absorbance at 300 nm).

The fact that TAL activity of the OsaPALs is significantly increased in the F → H mutations proves that this F residue is associated with substrate specificity as has been reported in some previous studies.[1,58] The compound, MIO, shown to be present in the crystal structure of PAL,[59] is believed to be involved in the PAL reaction as a cofactor attacking the carbon atom at the C2 position of the aromatic ring of L-Phe in a Friedel–Crafts-type reaction.[47] H134 and H128 of OsaPAL2F134H and OsaPAL62F128H, respectively, interact with the hydroxyl group of L-Tyr, resulting in an increase in affinity.[58] The hydroxyl group of L-Tyr also acts as an electron-donating group to increase the electron density at the C1, C3 and C5 positions of the aromatic ring,[60] thereby interfering with the attack by MIO; thus, the mutants retained higher catalytic activities towards L-Phe.[61]

3.7. Residue substitution successfully improves enzymes activity

The enzyme-kinetic properties of the purified proteins verified their biochemical function as *bona fide* OsaPALs, a finding which is expected to clarify the biosynthetic pathway of OSW-1. In addition, the successful characterization of the OsaPALs provides useful information for reconstructing the OSW-1 biosynthetic pathway and allows the scale-up of the production of OSW-1 using more active enzymes.

Following the successful functional characterization, the two sequences were aligned with three known PALs from yeasts together with other three PALs from plants (Fig. 11). The reason for selection of these PALs was that PALs from yeasts[61–63] appear to have higher catalytic activity than those from plants.[1,51,64] Examination of the sequence alignment revealed three residues around the ASG triad that were not absolutely conserved. The three amino acids are T, V, and G in plant PALs, whereas, in yeast PALs, the equivalent residues were S, S, and A. This is an interesting phenomenon that has not been reported to date in the literature. To identify the function of the three amino acids, site-directed mutagenesis was performed based on the consensus approach.[65–67]

The mutants were OsaPAL2T196S and OsaPAL62T194S, in which T196 of OsaPAL2 and T194 of OsaPAL62 were replaced with S; OsaPAL2V202S and OsaPAL62V200S, in which V202 of OsaPAL2 and V200 of OsaPAL62 were replaced with S; and OsaPAL2G209A and OsaPAL62G207A, in which G209 of OsaPAL2 and G207 of OsaPAL62 were replaced with A. In addition, two double mutants, OsaPAL2V202S/G209A and OsaPAL62V200S/G207A, and two triple mutants,

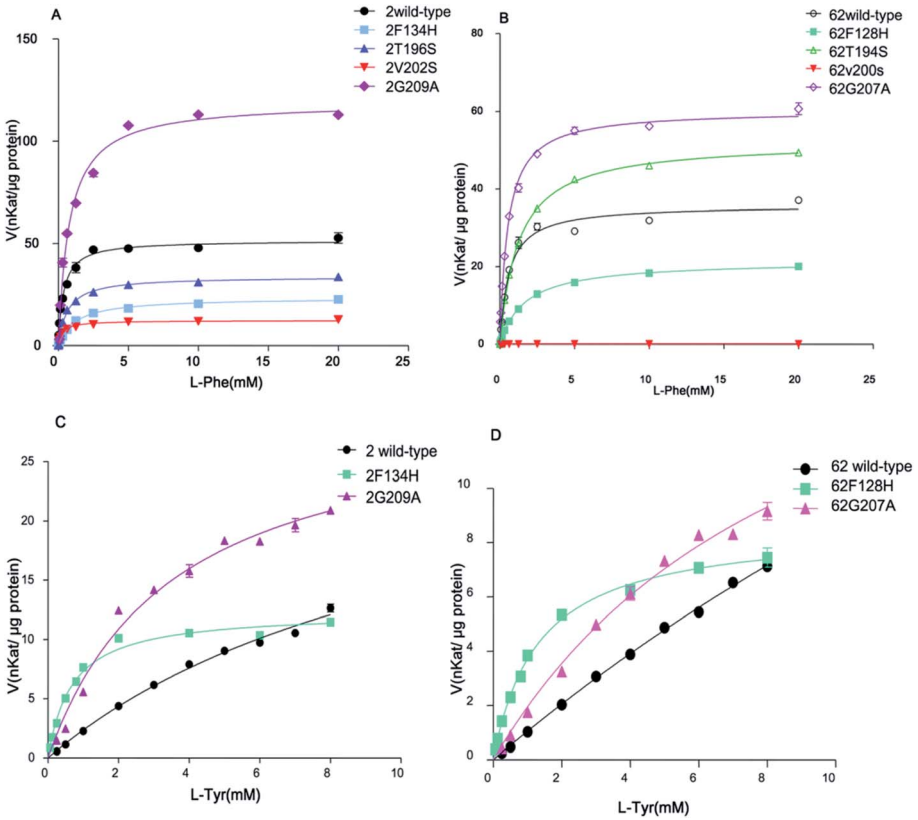

Fig. 8 Overlays of substrate saturation plots of different enzymes. (A andB) Plots of initial velocity against L-Phe concentration for reactions of wild-type and mutant enzymes. (C and D) Plots of initial velocity against L-Tyr concentration for reactions of wild-type and mutant enzymes. Wild-type enzymes did not reach enzyme saturation due to the limited solubility of L-Tyr.

OsaPAL2T196S/V202S/G209A and OsaPAL62T194S/V200S/G207A, were constructed.

After protein expression and purification (Fig. 12), the optimum pH and temperature for these mutants were determined to be the same as those for the wild proteins (ESI Fig. 1–3†). Then, the catalytic activities of these mutants were evaluated (Table 3 and Fig. 8–10), which reveal that although all the mutations lay near the PAL motif, their effects were diverse (Table 3). Using L-Phe as a substrate, both T → S mutations (OsaPAL2T196S and OsaPAL62T194S) and V → S

Table 3 Kinetic constants of OsaPAL2, OsaPAL62 and their mutants with L-Phe and L-Tyr as substrates. All assays were performed in aqueous 100 mM CHES (pH 9.5) at 44 °C. The formation of *trans*-cinnamic acid and *p*-coumaric acid were monitored continuously by multimode reader at 300 and 310 nm, respectively

Substrate	Enzyme	V_{max} (nkat per μg protein)	K_m (μM)	k_{cat} (s^{-1})	k_{cat}/K_m (M^{-1} s^{-1})
L-Phe	OsaPAL2	51.48 ± 0.82	371.5 ± 26.7	0.8025	2160
	OsaPAL2F134H	23.40 ± 0.23	1241 ± 44	0.3646	293.8
	OsaPAL2T196S	33.78 ± 0.36	662.9 ± 28.8	0.5264	794.1
	OsaPAL2V202S	12.21 ± 0.17	311.7 ± 21.1	0.1903	610.5
	OsaPAL2G209A	119.3 ± 2.2	790.4 ± 57.54	1.861	2354
	OsaPAL62	35.82 ± 0.70	593.1 ± 48.6	0.5545	934.9
	OsaPAL62F128H	21.5 ± 0.2	1679 ± 43	0.3328	198.2
	OsaPAL62T194S	52.27 ± 0.46	1236 ± 39	0.8105	655.7
	OsaPAL62V200S	0.08034 ± 0.00130	118.9 ± 10.4	0.0003105	2.612
	OsaPAL62G207A	60.26 ± 0.61	529.2 ± 23.0	0.9332	1763
L-Tyr	OsaPAL2	29.73 ± 2.41	11690 ± 1410	0.4635	39.65
	OsaPAL2F134H	12.35 ± 0.23	691.0 ± 46.0	0.1925	278.6
	OsaPAL2G209A	30.08 ± 1.33	3538 ± 365	0.4690	132.6
	OsaPAL62	42.35 ± 4.40	39280 ± 472	0.6557	16.69
	OsaPAL62F128H	8.603 ± 0.161	1320 ± 74	0.1332	100.9
	OsaPAL62G207A	20.29 ± 1.56	9423 ± 1148	0.3143	33.35

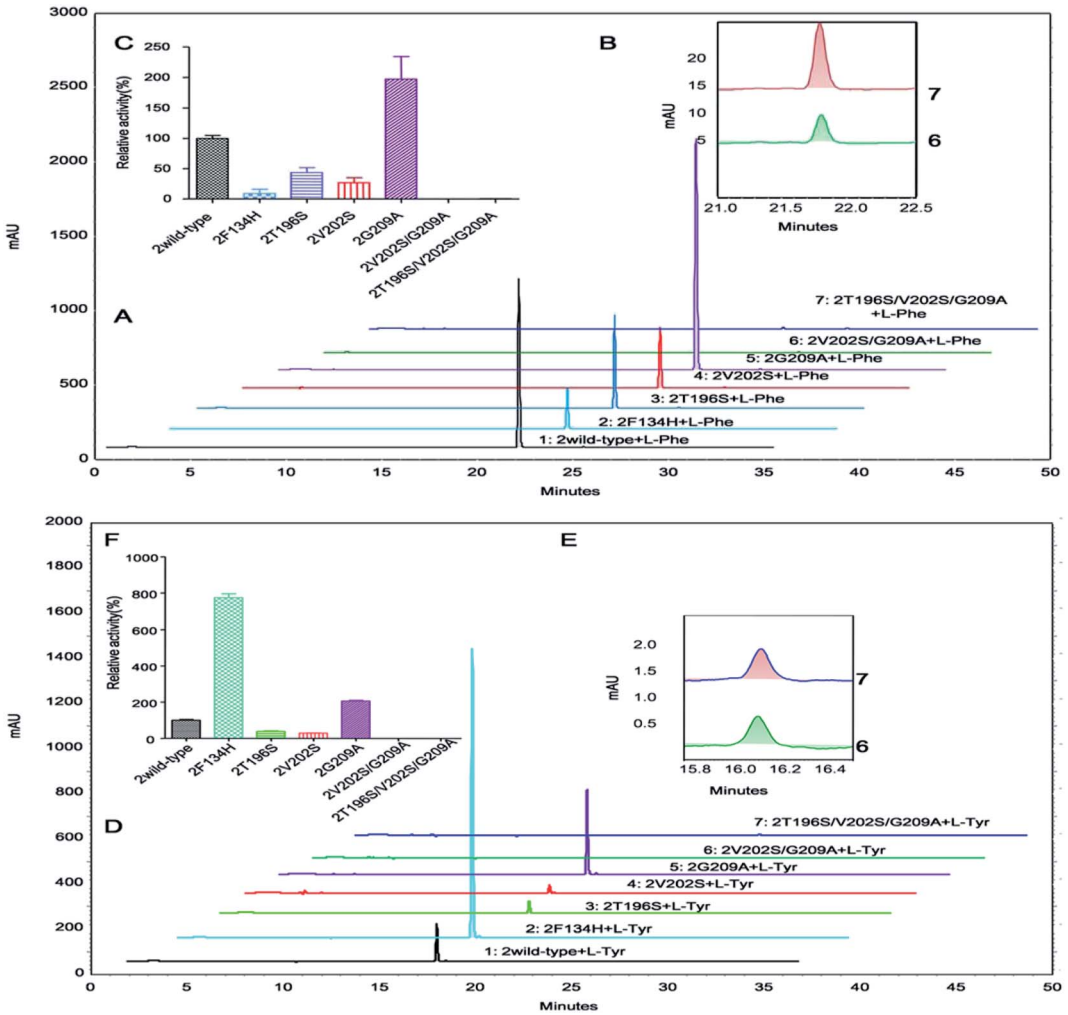

Fig. 9 Comparison of OsaPAL2 mutant and wild-type activities. (A and D) HPLC was used to compare OsaPAL2 wild-type and mutant activities using the same amount of purified enzyme and substrate L-Phe or L-Tyr in an aqueous buffer. The data is for a reaction lasting 3 h with the various heights indicating the different amounts of products (Note that the UV absorption of the product of L-Phe was high at 275 nm producing flat-topped peaks. To improve the precision of the results, we also monitored the absorbance at 300 nm.) (B and E) Partially enlarged views of 2V202S/G209A and 2T196S/V202S/G209A. (C and F) Relative activity was determined based on an average rate of 9 independent experiments; scale was set to 100% for wild-type OsaPAL2. Results are presented as means ± SD.

mutations (OsaPAL2V202S and OsaPAL62V200S) exhibited lower catalytic efficiency with values of k_{cat}/K_m lower than those of the wild-type enzymes, in particular of OsaPAL62V200S whose k_{cat}/K_m value was only 0.33% of that of OsaPAL62.

Interestingly, the T → S mutation, where one hydrophilic amino acid replaces another, showed lower affinity with K_m values 2-fold higher and lower catalytic efficiency compared to the wild-type. In contrast, the V → S mutation, where a hydrophilic amino acid replaces a hydrophobic one, showed higher affinity than the wild-type. Furthermore, the G → A mutants were did not exhibit significant difference in affinity; however, they exhibited higher catalytic efficiency than the wild type.

The double mutants OsaPAL2V202S/G209A and OsaPAL62V200S/G207A exhibited activities too low to be detected by the multimode reader; however, by HPLC analysis, they were shown to have activities that were only 0.006% and 0.129%, respectively, of the wild-type activities for L-Phe (Fig. 9 and 10). The introduction of a third mutation to afford the triple mutants OsaPAL2T196S/V202S/G209A and OsaPAL62T194S/V200S/G207A restored some degree of activity for L-Phe (0.016–0.339%) (Fig. 9 and 10). The relative activities of other mutants were also evaluated by HPLC and shown to be consistent with their kinetic constants. In brief, the activity of OsaPAL2G209A and OsaPAL62G207A was highest, followed by the wild-type, followed by OsaPAL2T196S and OsaPAL62T194S with slightly lower activity than the wild-type, and finally OsaPAL2V202S and OsaPAL62V200S. Activities of the double mutants OsaPAL2V202S/G209A and OsaPAL62V200S/G207A and triple mutants OsaPAL2T196S/V202S/G209A and OsaPAL62T194S/V200S/G207A were negligible. Similar results were obtained by HPLC for L-Tyr deamination activity (Fig. 9 and 10).

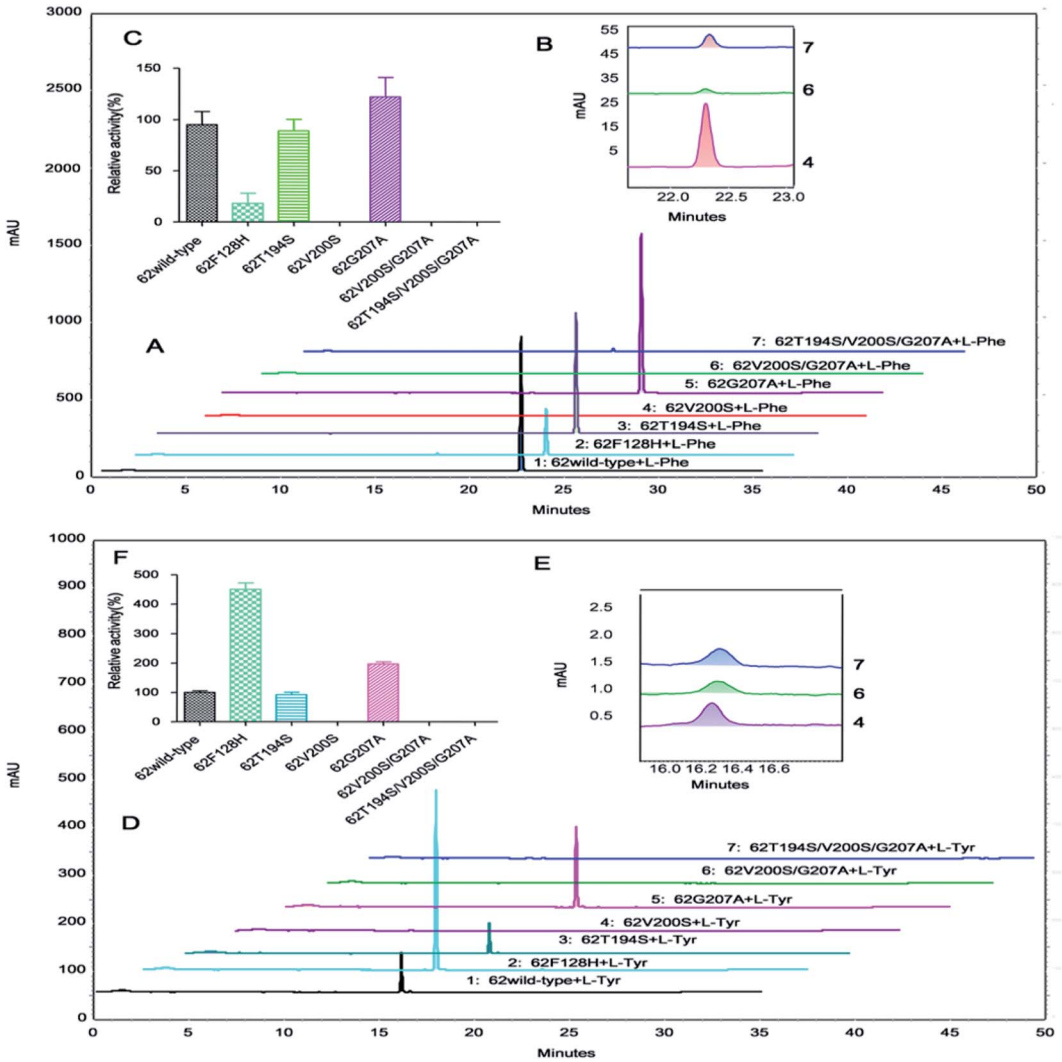

Fig. 10 Comparison of OsaPAL62 mutant and wild-type activities. (A and D) HPLC was used to compare OsaPAL62 wild-type and mutant activities using the same amount of purified enzymes and substrate L-Phe or L-Tyr in an aqueous buffer. The data is for a reaction lasting 3 h with the various heights indicating the different amount of products. (Note UV absorption of the product of L-Phe was high at 275 nm producing flat-topped peaks. To improve the precision of the results, we also monitored the absorbance at 300 nm). (B and E) Partially enlarged views of 62V200S, 62V200S/G207A and 62T194S/V200S/G207A. (C and F) Relative activity is presented as a mean ± SD of 9 independent experiments, scale was set to 100% for the wild-type OsaPAL62.

In both of the two proposed reaction mechanisms for PAL,[48,60,68,69] the A–S–G triad in the motif can rearrange to a MIO ring to attack substrates. The importance of the triad has been demonstrated in many studies but little research has focused on other conserved amino acids around it.

The results described above indicate that residues adjacent to the A–S–G triad may play different roles. In considering the K_m values of single mutants in relation to the positions of mutations, the higher affinity but lower catalytic efficiency of OsaPAL2V202S and OsaPAL62V200S suggests that the S202 in the former and S200 in the latter may form hydrogen bonds with the β-proton of the substrate and hinder its elimination. However, the elucidation of the exact mechanism needs further investigation.

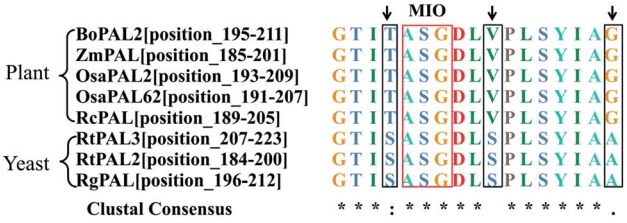

Fig. 11 Multiple alignments of PAL signatures of plants and yeasts. The red box highlights the active site motif (A–S–G), which undergoes autocatalysis to form MIO. The residues that differ in yeasts and plants are shown in black boxes. The sequences used are OsaPAL2, OsaPAL62, *Rhus chinensis* RcPAL (AGH13333), *Zea mays* ZmPAL (NP_001105334), *Bambusa oldhamii* BoPAL2 (ACN62413.1), *Rhodotorula glutinis JN-1* RgPAL (see ref. 61), *Rhodosporidium toruloides* RtPAL3 (P11544), *Rhodosporidium toruloides* RtPAL2 (AAA33883.1).

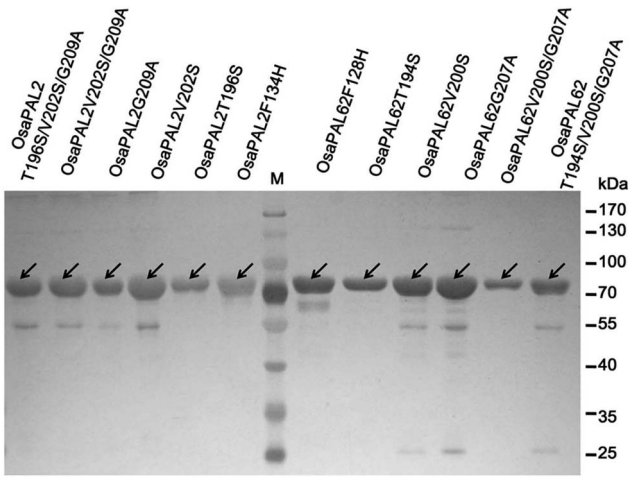

Fig. 12 SDS-PAGE analysis of purified mutants of OsaPAL2 and OsaPAL62. M stands for protein standards with corresponding molecular weights shown on the right; small black arrows indicate target proteins with similar molecular weights.

4. Conclusions

4.1. First functional characterization of PAL cDNAs from Asparagaceae plant species

PALs are fairly ubiquitous in plants, including monocots, dicots, gymnosperms, ferns, lycopods, liverworts, and algae; however, there are no reports about PALs from Asparagaceae plant species.

4.2. The function of three amino acids around ASG triad

PALs from yeasts appear to have a higher catalytic activity than those from plants. The examination of the sequence alignment revealed three residues around the ASG triad that were not absolutely conserved. The three amino acids are T, V, and G in the plant PALs, whereas in yeast PALs, the equivalent residues were S, S, and A. The amino acid difference may be the reason for the discrepancy in catalytic activity between plant PALs and yeast PALs. Mutagenesis studies demonstrated that the Thr-to-Ser mutants, OsaPAL2T196S and OsaPAL62T194S showed significantly higher substrate affinity than the wild-types; moreover, the Gly-to-Ala mutants, OsaPAL2G209A and OsaPAL62G207A showed higher PAL and TAL activities. To the best of our knowledge, this is the first report about these three mutants. It is also the first time that we have improved both PAL and TAL activities by a single amino acid substitution.

4.3. The function of phenylalanine as a substrate selective switch

There are some confusing results about the function of Phe as a substrate selective switch. In the paper presented by Watts *et al.*,[58] when Phe144 residue was replaced by His in *A. thaliana* PAL1, the mutant displayed a marked reduction (80-fold) in k_{cat}/Km value together with an 18-fold increase in the catalytic efficiency towards tyrosine. This result clearly showed that Phe144 controlled the substrate selection; however, this was not the case in the report published by Hsieh *et al.*[51] When Phe133 was substituted with His, a slightly increased k_{cat}/Km value toward tyrosine was found in the F133H mutant. They inferred that other residues also contribute to the substrate selectivity of PALs. To further clarify the function of phenylalanine, two mutants OsaPAL2F134H and OsaPAL62F128H were produced by site-directed mutagenesis. The results corroborated that Phe does indeed control substrate selection.

Acknowledgements

This work was supported by National Mega-project for Innovative Drugs (no. 2012ZX09301002), Open Foundation of State Key Laboratory of Bioactive Substance and Function of Natural Medicines (B-2011-4) and PUMC Youth Fund (2012J21, 3332013112).

References

1 A. B. Oliveira, C. F. Moura, E. Gomes-Filho, C. A. Marco, L. Urban and M. R. Miranda, *PLoS One*, 2013, **8**, e56354.
2 J. Song and Z. Wang, *Mol. Biol. Rep.*, 2009, **36**, 939–952.
3 Y. Mimaki, M. Kuroda, A. Kameyama, Y. Sashida, T. Hirano, K. Oka, R. Maekawa, T. Wada, K. Sugita and J. A. Beutler, *Bioorg. Med. Chem. Lett.*, 1997, **7**, 633–636.
4 K. Tamura, H. Honda, Y. Mimaki, Y. Sashida and H. Kogo, *Br. J. Pharmacol.*, 1997, **121**, 1796–1802.
5 Y. Zhou, C. Garcia-Prieto, D. A. Carney, R. H. Xu, H. Pelicano, Y. Kang, W. Yu, C. Lou, S. Kondo, J. Liu, D. M. Harris, Z. Estrov, M. J. Keating, Z. Jin and P. Huang, *J. Natl. Cancer Inst.*, 2005, **97**, 1781–1785.
6 S. Deng, B. Yu, Y. Lou and Y. Hui, *J. Org. Chem.*, 1999, **64**, 202–208.
7 J. W. Morzycki and A. Wojtkielewicz, *Carbohydr. Res.*, 2002, **337**, 1269–1274.
8 M. Tsubuki, S. Matsuo and T. Honda, *Tetrahedron Lett.*, 2008, **49**, 229–232.
9 W. Yu and Z. Jin, *J. Am. Chem. Soc.*, 2002, **124**, 6576–6583.
10 J. Xue, P. Liu, Y. Pan and Z. Guo, *J. Org. Chem.*, 2008, **73**, 157–161.
11 S. Kubo, Y. Mimaki, M. Terao, Y. Sashida, T. Nikaido and T. Ohmoto, *Phytochemistry*, 1992, **31**, 3969–3973.
12 M. Kuroda, Y. Mimaki, A. Yokosuka, F. Hasegawa and Y. Sashida, *J. Nat. Prod.*, 2002, **65**, 1417–1423.
13 M. Kuroda, Y. Mimaki, A. Yokosuka, Y. Sashida and J. A. Beutler, *J. Nat. Prod.*, 2001, **64**, 88–91.
14 A. Podstolski, D. Havkin-Frenkel, J. Malinowski, J. W. Blount, G. Kourteva and R. A. Dixon, *Phytochemistry*, 2002, **61**, 611–620.
15 D. Sircar and A. Mitra, *J. Plant Physiol.*, 2009, **166**, 1370–1380.
16 R. Loscher and L. Heide, *Plant Physiol.*, 1994, **106**, 271–279.
17 J. Koukol and E. E. Conn, *J. Biol. Chem.*, 1961, **236**, 2692–2698.
18 X. Hou, F. Shao, Y. Ma and S. Lu, *Mol. Biol. Rep.*, 2013, **40**, 4301–4310.
19 C. J. Dong and Q. M. Shang, *Planta*, 2013, **238**, 35–49.

20 S. Giberti, C. M. Bertea, R. Narayana, M. E. Maffei and G. Forlani, *J. Plant Physiol.*, 2012, **169**, 249–254.
21 H. Yoon, Y. H. You, Y. E. Kim, Y. J. Kim, W. S. Kong and J. G. Kim, *J. Microbiol. Biotechnol.*, 2013, **23**, 1055–1059.
22 C. A. Vaslet, R. L. Strausberg, A. Sykes, A. Levy and D. Filpula, *Nucleic Acids Res.*, 1988, **16**, 11382.
23 C. W. Abell and R. S. Shen, *Methods Enzymol.*, 1987, **142**, 242–253.
24 K. Kovacs, G. Banoczi, A. Varga, I. Szabo, A. Holczinger, G. Hornyanszky, I. Zagyva, C. Paizs, B. G. Vertessy and L. Poppe, *PLoS One*, 2014, **9**, e85943.
25 J. S. Williams, M. Thomas and D. J. Clarke, *Microbiology*, 2005, **151**, 2543–2550.
26 M. C. Moffitt, G. V. Louie, M. E. Bowman, J. Pence, J. P. Noel and B. S. Moore, *Biochemistry*, 2007, **46**, 1004–1012.
27 X. H. Wang, M. Gong, L. Tang, S. Zheng, J. D. Lou, L. Ou, J. Gomes-Laranjo and C. Zhang, *Mol. Biol. Rep.*, 2013, **40**, 97–107.
28 Q. Jin, Y. Yao, Y. Cai and Y. Lin, *PLoS One*, 2013, **8**, e62352.
29 Y. Jiang, B. Xia, L. Liang, X. Li, S. Xu, F. Peng and R. Wang, *Mol. Biol. Rep.*, 2013, **40**, 2293–2300.
30 C. Fang, Y. Zhuang, T. Xu, Y. Li, Y. Li and W. Lin, *J. Chem. Ecol.*, 2013, **39**, 204–212.
31 F. Xu, G. Deng, S. Cheng, W. Zhang, X. Huang, L. Li, H. Cheng, X. Rong and J. Li, *Molecules*, 2012, **17**, 7810–7823.
32 U. R. Bagal, J. H. Leebens-Mack, W. W. Lorenz and J. F. Dean, *BMC Genomics*, 2012, **13**, 1–9.
33 W. H. Xiao, J. S. Cheng and Y. J. Yuan, *J. Biotechnol.*, 2009, **139**, 222–228.
34 R. W. Whetten and R. R. Sederoff, *Plant Physiol.*, 1992, **98**, 380–386.
35 G. Hao, X. Du, F. Zhao and H. Ji, *Biotechnol. Lett.*, 2010, **32**, 305–314.
36 M. R. Young, G. H. N. Towers and A. C. Neish, *Can. J. Bot.*, 1966, **44**, 341–349.
37 U. Czichi and H. Kindi, *Hoppe-Seyler's Z. Physiol. Chem.*, 1975, **356**, 475–485.
38 I. A. Veliky and S. M. Martin, *Can. J. Microbiol.*, 1970, **16**, 223–226.
39 J. Q. Kong, D. Lu and Z. B. Wang, *Molecules*, 2014, **19**, 1608–1621.
40 Y. Wei, J. Thompson and C. Floudas, *Proc. R. Soc. A*, 2012, **468**, 831–850.
41 M. A. Larkin, G. Blackshields, N. P. Brown, R. Chenna, P. A. McGettigan, H. McWilliam, F. Valentin, I. M. Wallace, A. Wilm, R. Lopez, J. D. Thompson, T. J. Gibson and D. G. Higgins, *Bioinformatics*, 2007, **23**, 2947–2948.
42 K. Tamura, D. Peterson, N. Peterson, G. Stecher, M. Nei and S. Kumar, *Mol. Biol. Evol.*, 2011, **28**, 2731–2739.
43 A. Kumar and B. E. Ellis, *Plant Physiol.*, 2001, **127**, 230–239.
44 F. C. Cochrane, L. B. Davin and N. G. Lewis, *Phytochemistry*, 2004, **65**, 1557–1564.
45 R. Shi, C. M. Shuford, J. P. Wang, Y. H. Sun, Z. Yang, H. C. Chen, S. Tunlaya-Anukit, Q. Li, J. Liu, D. C. Muddiman, R. R. Sederoff and V. L. Chiang, *Planta*, 2013, **238**, 487–497.
46 J. Kyte and R. F. Doolittle, *J. Mol. Biol.*, 1982, **157**, 105–132.
47 L. Poppe, *Curr. Opin. Chem. Biol.*, 2001, **5**, 512–524.
48 L. Poppe and J. Retey, *Angew. Chem., Int. Ed.*, 2005, **44**, 3668–3688.
49 J. Retey, *Biochim. Biophys. Acta*, 2003, **1647**, 179–184.
50 L. S. Hsieh, G. J. Ma, C. C. Yang and P. D. Lee, *Phytochemistry*, 2010, **71**, 1999–2009.
51 J. Rosler, F. Krekel, N. Amrhein and J. Schmid, *Plant Physiol.*, 1997, **113**, 175–179.
52 Z. M. Gao, X. C. Wang, Z. H. Peng, B. Zheng and Q. Liu, *Plant Cell Rep.*, 2012, **31**, 1345–1356.
53 J. D. Cui, L. L. Li and H. J. Bian, *PLoS One*, 2013, **8**, e80581.
54 J. Jorrin, R. Lopez-Valbuena and M. Tena, *Biochem. Int.*, 1991, **24**, 1–11.
55 A. D. Sarma and R. Sharma, *Phytochemistry*, 1999, **50**, 729–737.
56 J. Gao, S. Zhang, F. Cai, X. Zheng, N. Lin, X. Qin, Y. Ou, X. Gu, X. Zhu, Y. Xu and F. Chen, *Mol. Biol. Rep.*, 2012, **39**, 3443–3452.
57 K. T. Watts, B. N. Mijts, P. C. Lee, A. J. Manning and C. Schmidt-Dannert, *Chem. Biol.*, 2006, **13**, 1317–1326.
58 G. V. Louie, M. E. Bowman, M. C. Moffitt, T. J. Baiga, B. S. Moore and J. P. Noel, *Chem. Biol.*, 2006, **13**, 1327–1338.
59 J. C. Calabrese, D. B. Jordan, A. Boodhoo, S. Sariaslani and T. Vannelli, *Biochemistry*, 2004, **43**, 11403–11416.
60 B. Schuster and J. Rétey, *Proc. Natl. Acad. Sci. U. S. A.*, 1995, **92**, 8433–8437.
61 L. Zhu, W. Cui, Y. Fang, Y. Liu, X. Gao and Z. Zhou, *Biotechnol. Lett.*, 2013, **35**, 751–756.
62 I. L. Bazukian, A. E. Vardanian, A. A. Ambartsumian, P. V. Tozalakian and G. Popov Iu, *Prikl. Biokhim. Mikrobiol.*, 2009, **45**, 23–27.
63 C. T. Evans, K. Hanna, D. Conrad, W. Peterson and M. Misawa, *Appl. Microbiol. Biotechnol.*, 1987, **25**, 406–414.
64 L. S. Hsieh, C. S. Yeh, H. C. Pan, C. Y. Cheng, C. C. Yang and P. D. Lee, *Protein Expression Purif.*, 2010, **71**, 224–230.
65 M. Lehmann and M. Wyss, *Curr. Opin. Biotechnol.*, 2001, **12**, 371–375.
66 R. A. Chica, N. Doucet and J. N. Pelletier, *Curr. Opin. Biotechnol.*, 2005, **16**, 378–384.
67 S. Lutz, *Curr. Opin. Biotechnol.*, 2010, **21**, 734–743.
68 K. R. Hanson and E. A. Havir, *Arch. Biochem. Biophys.*, 1970, **141**, 1–17.
69 J. D. Hermes, P. M. Weiss and W. W. Cleland, *Biochemistry*, 1985, **24**, 2959–2967.